PERGAMON

Journal of Structural Geology 21 (1999) 1219–1227

JOURNAL OF STRUCTURAL GEOLOGY

www.elsevier.nl/locate/jstrugeo

# Are feldspar-to-mica reactions necessarily reaction-softening processes in fault zones?

Christopher Wibberley*

*Laboratoire de Géophysique et Tectonique, Case 060, Université Montpellier II, Place E. Bataillon, 34095 Montpellier, France*

Received 1 April 1998; accepted 3 December 1998

**Abstract**

Reaction-softening by mineralogical changes from feldspars to sericite has been documented from many fault zones. During external crystalline basement deformation in the Alpine orogeny, the Ser Barbier thrust and splay faults in the Pelvoux Massif experienced ultracataclasis and sericitisation. Microstructural information and geochemical data from the fault rocks suggest that different muscovitisation reactions occurred at different times within the evolution of the fault zone, and each reaction had its own impact on fault rheology. Early cataclasis aided chemical breakdown of orthoclase feldspars to muscovite, yet quartz release accompanying this process resulted in local cementation and consequent *hardening* of the ultracataclasite. Continued deformation was accompanied by muscovitisation of the albite feldspar, and resulted in the formation of mica-rich fault rocks which experienced progressive silica removal by the fluid with increasing deformation. At this stage, reaction-enhanced ductility dominated. Much of the early cemented ultracataclasites escaped later deformation, and their low permeability allowed preservation of their early geochemical characteristics by preventing later fluid access. Such findings demonstrate how the complex interplay between deformation processes and geochemical reactions may result in a changing rheology during fault zone evolution. 

## 1. Introduction

Geochemical reactions in fault zones are generally fluid induced and are commonly suggested to result in changes in fault rock rheology. Most of these changes are reaction-softening effects (e.g. White and Knipe, 1978; Brodie and Rutter, 1985; Rubie, 1990) and the breakdown of relatively strong feldspars to easily deformable phyllosilicates is one of the most commonly reported. At lower greenschist facies conditions, feldspar breakdown to white mica commonly occurs. This process has often been suggested to be an important reaction-softening step in granitic fault zones (e.g. O'Hara, 1988; Evans, 1990; Mitra, 1992; Evans and Chester, 1995; Wintsch et al., 1995), and has also been suggested to be a explanation for anomalously low friction on the San Andreas Fault (Evans and Chester, 1995; Wintsch et al., 1995).

### 1.1. The feldspar muscovitisation reactions

The breakdown reactions of albite and orthoclase to fine-grained muscovite (often called sericite) may be represented by the following equations (Hemley and Jones, 1964), written to conserve aluminium:

$$3NaAlSi_3O_8 + K^+ + 2H^+ \rightarrow KAl_3Si_3O_{10}(OH)_2 + 6SiO_2 + 3Na^+$$

albite→muscovite + silica

$$3KAlSi_3O_8 + 2H^+ \rightarrow KAl_3Si_6O_{10}(OH)_2 + 6SiO_2 + 2K^+ \quad (2)$$

orthoclase→muscovite + silica

* Present address: Department of Geology and Mineralogy, Division of Earth and Planetary Sciences, Graduate School of Science, Kyoto University, Kitashirukawa-oiwoke cho, Kyoto 606-8502, Japan.

*E-mail address:* wibbs@dstu.univ-montp2.fr (C. Wibberley)

0191-8141/99/$ - see front matter 
PII: S0191-8141(99)00019-X

These equations demonstrate the requirement of an acidic fluid for muscovitisation to occur. Temperature, pressure and fluid composition may govern the reactions and phase stability in the albite–orthoclase–muscovite system, and this has been demonstrated with the use of $(a_{Na^+}/a_{H^+})$ vs $(a_{K^+}/a_{H^+})$ activity plots (e.g. Wintsch, 1975a).

### *1.2. Interplay between deformation and muscovitisation reactions*

Feldspar muscovitisation reactions play an important role in deformation processes (e.g. White and Knipe, 1978; Knipe and Wintsch, 1985). The most noted way is by reaction-enhanced ductility (White and Knipe, 1978), where relatively strong feldspars [at temperatures less than, say, 500°C (e.g. Voll, 1976; Tullis, 1983 and many others)] are replaced by micas, which are much more easily deformed (e.g. Shea and Kronenberg, 1993). This has been documented in basement rocks both in cataclastic fault zones (e.g. Janecke and Evans, 1988; Evans, 1990; Mitra, 1992) and in mylonitic shear zones (e.g. Knipe and Wintsch, 1985; O'Hara, 1988; Imber et al., 1997). Wintsch (1978) describes evidence for syntectonic mica growth perpendicular to $\sigma_1$ by dissolution of quartz and feldspar, and later by recrystallisation of earlier formed phyllosilicates. Micas deform relatively easily by grain boundary sliding, cleavage plane slip, and dislocation glide, and the (001) plane in micas is important in crystal 'stacking faults' (Bell and Wilson, 1981). Hence the formation of an aligned mica foliation weakens the tectonite (e.g. Wintsch et al., 1995). Given the common occurrence of aligned sericite in basement fault zones (e.g. Wibberley, 1995), this makes muscovitisation and consequent reaction-softening an especially important process. In prograde situations, the reactions in Eqs. (1) and (2) may operate in reverse (Wintsch, 1975b) resulting in reaction hardening (Wintsch et al., 1995).

Hence the behaviour of a fault zone subsequent to reaction is a direct result of the rheology of the products of the particular reactions taking place. However, deformation can control the occurrence and location of these reactions in the first place. For example, Knipe and Wintsch (1985) describe how deformation influences the operation and reaction direction of feldspar ↔ muscovite reactions by enhancing (1) source solubility (e.g. by generating new reaction surfaces by fracturing), (2) pathways (e.g. by grain-size reduction) and (3) sinks (e.g. by void formation).

In this way, muscovitisation reactions can both facilitate, and be facilitated by, deformation. I aim to illustrate possible relationships between muscovitisation and the evolution of deformation mechanisms operating in granitic basement fault zones, using data from the Ser Barbier thrust sheet. Relevance to consequent hardening and softening will be emphasised.

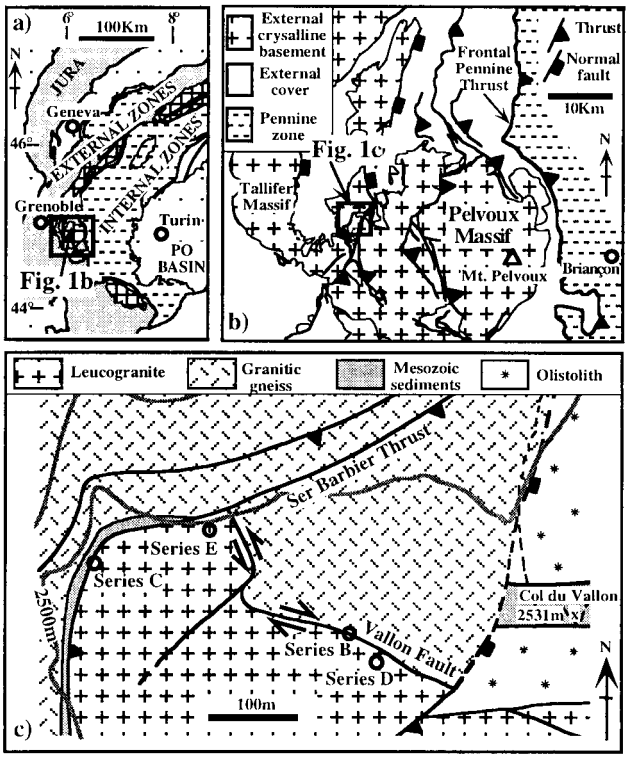


Fig. 1. Structural setting of the study area. (a) The Western Alps. (b) Map of the Pelvoux Massif, with location of the study area. (c) Simplified geological map of the study area, with positions of the sampling sites.

## 2. Regional setting

The Pelvoux Massif (Fig. 1a, b) consists of a series of crystalline thrust sheets emplaced during neo-Alpine deformation and greenschist-grade metamorphism (e.g. Frey et al., 1974). On the Northwest side of the Pelvoux Massif, the Ser Barbier Thrust (Fig. 1c) emplaced crystalline basement to the WNW over Mesozoic cover (Wibberley, 1995) under low greenschist facies conditions ($T \sim 300°$, $P \sim 180$ MPa, Jullien and Goffé, 1993). The basement-on-cover thrust relationship demonstrates an Alpine age for the Ser Barbier thrust zone. The crystalline basement in this part of the Pelvoux Massif is generally Precambrian granitic gneiss and leucogranite with a composition of quartz–albite–orthoclase (Barféty et al., 1988). Within the Ser Barbier thrust sheet, the Vallon transfer fault strikes WNW–ESE (parallel to the emplacement direction) and divides the thrust sheet into two compartments which were emplaced different magnitudes along the Ser Barbier Thrust (Wibberley, 1997), thereby suggesting that it also has an Alpine age of fault activity. This is corroborated by the close similarity in

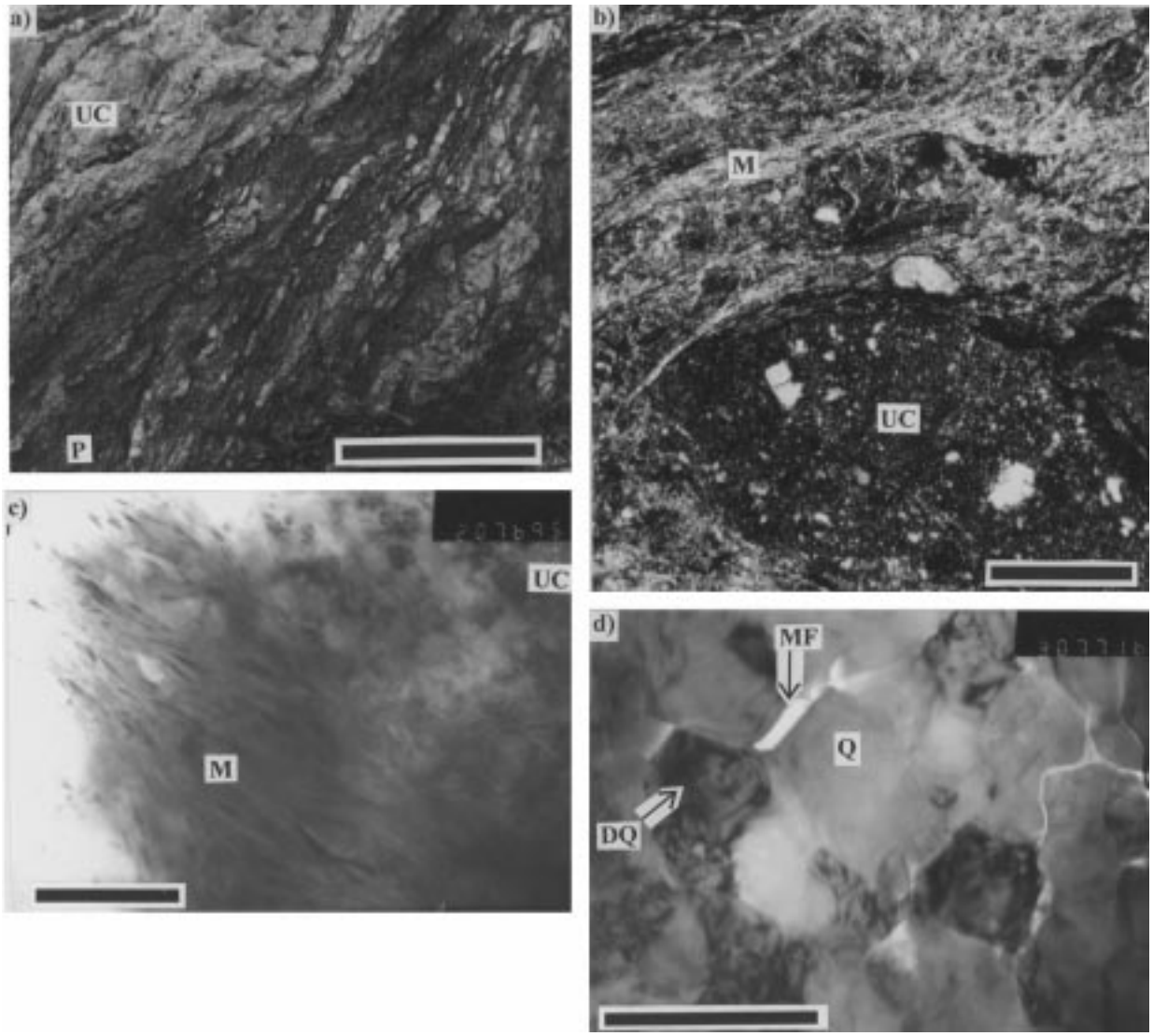


Fig. 2. Textures and microtextures of the Alpine fault rocks: (a) Field photograph of the Vallon Fault zone showing the fabric of the black phyllonites (P), and white cemented ultracataclasite zones (UC). Scale bar represents 15 cm. (b) Optical micrograph of a phyllonite sample from the Vallon Fault zone, showing the muscovite fabric (M) wrapping around a microclast of cemented quartz–albite ultracataclasite (UC). Scale bar represents 0.5 mm. (c) Transmission electron micrograph of a phyllonite sample from the Ser Barbier thrust, showing a narrow zone of aligned muscovite (M) cutting through welded ultracataclasite (UC). Scale bar represents 1 μm. (d) Transmission electron micrograph of cemented ultracataclasite, showing closely packed quartz and feldspar typical of a low-porosity welded cataclasite (e.g. Knipe, 1990) with both dislocated quartz grains (DQ) and relatively strain-free quartz grains (Q). A single void (MF) was probably due to a mica flake falling out during TEM foil preparation. Scale bar represents 1 μm.

fault zone chemistry and microstructures between the Alpine Ser Barbier Thrust and the Vallon Fault (Wibberley, 1995).

The wall rocks to these faults have an orthoclase-to-albite ratio varying from 1:1 to 2:1, and small amounts of sericite and chlorite appear as alteration products around zones of microfracturing. This alteration becomes more marked close to small splay faults which branch off the main fault zones described, and so is considered also to be Alpine in age. This implies that these rocks do not truely have the same composition as the initial protolith to the fault zones, but are considered to be 'least altered equivalents'.

## 3. Observational data

### 3.1. Macroscale fault rock textures

The Ser Barbier Thrust and the Vallon Fault zones are both 1–4 m wide and contain mostly black (iron-stained) strongly foliated phyllonites (e.g. Fig. 2a).

This foliation is defined by the strong preferred alignment of secondary fine-grained sericite mica. However, within these phyllonitic fault zones, lumps or bands of white cemented ultracataclastite are present. These ultracataclastic fault rocks do not have a fabric visible in the field and are very resistant to weathering and hammering, unlike the weak phyllonites. They pre-date the black phyllonites as the fault phyllonite foliation cross-cuts or wraps around zones of white cemented ultracataclasite within the fault zones. The wall rocks to these fault zones are of leucogranitic composition in the areas sampled. A more detailed structural analysis is given by Wibberley (1995).

### 3.2. Petrographic data

Samples of the two types of fault rock visible in the field have been examined by optical, backscattered scanning electron and transmission electron microscopy. Modal compositions of the fault rocks were assessed by very detailed point counting from large SEM images of suitable coverage and scale. The following values are averages:

Cemented ultracataclasite: 33% quartz, 7% orthoclase, 24% albite, 29% muscovite.
Phyllonite: 22% quartz, 12% orthoclase, 7% albite, 52% muscovite.

In each case, small ($<5\%$) amounts of chlorite, calcite and iron oxide are also present, making up the remainder of the percentage. It is clear from this petrographic data that the cemented ultracataclasites have far less orthoclase and more muscovite than the least altered equivalent. The phyllonites have far less albite as well as less orthoclase than the least altered equivalent, but more muscovite. Furthermore, the phyllonites have less albite but more muscovite than the ultracataclasites.

### 3.3. Microtextural data

Under the optical microscope, an aligned fine-grained secondary white mica foliation is seen to wrap around microclasts of cemented quartz–feldspar ultracataclasite (Fig. 2b), thus the fabric post-dates the ultracataclasite. This micaceous fabric dominates the fault zones. The white mica exists either as narrow ($\sim$10 μm wide) seams within feldspar- and quartz-rich domains or in wider mica-rich regions up to 1 mm thick which are contiguous and anastomose around the mica-poor regions. Quantitative microprobe data on the white mica show a muscovitic composition with only a small iron content, unlike the phengitic compositions of sericites described from many retrograde fault zones. Wall rock and fault zone feldspar compositions are similarly determined, and found to be close to pure orthoclase and pure albite.

Fig. 2(c) illustrates that domains of quartz-rich cemented ultracataclasite are cut by closely packed aligned muscovite zones even at the micron scale, within a phyllonite sample. This suggests that parts of the ultracataclasite were broken down during the evolution of the phyllonite. The abundance of aligned muscovite in the phyllonite suggests that ductile deformation mechanisms soon dominated phyllonite development during progressive muscovite formation. The muscovite in this example exhibits relatively low strain, and grew relatively late in the activity of the fault zone. Fig. 2(d) shows a cemented ultracataclasite 1 cm from the Ser Barbier thrust contact, consisting of quartz and albite with a typical grain size of 0.25–0.5 μm. The grains fit tightly together and porosity is absent, suggesting an extremely low permeability in the absence of further fracturing. Dislocated clasts exist within the cement, generally $\sim$0.5 μm in diameter, with much more irregular grain shapes than the cementing grains. The hexagonal shape and arrangement of quartz grains in this sample reflects the fluid-assisted local redistribution of silica due to grain-scale compaction during deformation. Other nearby areas are dilatant sites of growth of new quartz, and this texture is typical of cemented cataclasites from faults in quartz-rich lithologies (e.g. Knipe, 1990). The probable low permeability in these cemented regions (cf. Fig. 2d) means that further alteration would be unlikely to occur within the cemented domains of the ultracataclasite, unless later fractures are present within the rock to allow fluid infiltration.

In summary, the fault phyllonite was produced by the breakdown of earlier quartz–albite ultracataclasite accompanied by growth of muscovite. The petrographic data suggest that this mica was produced at the expense of albite feldspar. For the ultracataclasite, imaging of reaction textures was difficult due to the fine grain size and the abundance of quartz. However, it is clear that ultracataclasite formation was accompanied by significant quartz growth and consequent cementation.

## 4. Geochemical data

In this section, I present major element and selected trace element geochemical data (whole rock XRF) on samples taken from both the basement fault zones (ultracataclasite and phyllonite samples) and the 'least altered equivalent' wall rock. Data are presented in the form of major element oxide weight percentages and trace element concentrations. Only a brief resumé of the data is presented here, but a more complete presentation of the data is given in Wibberley (1995).

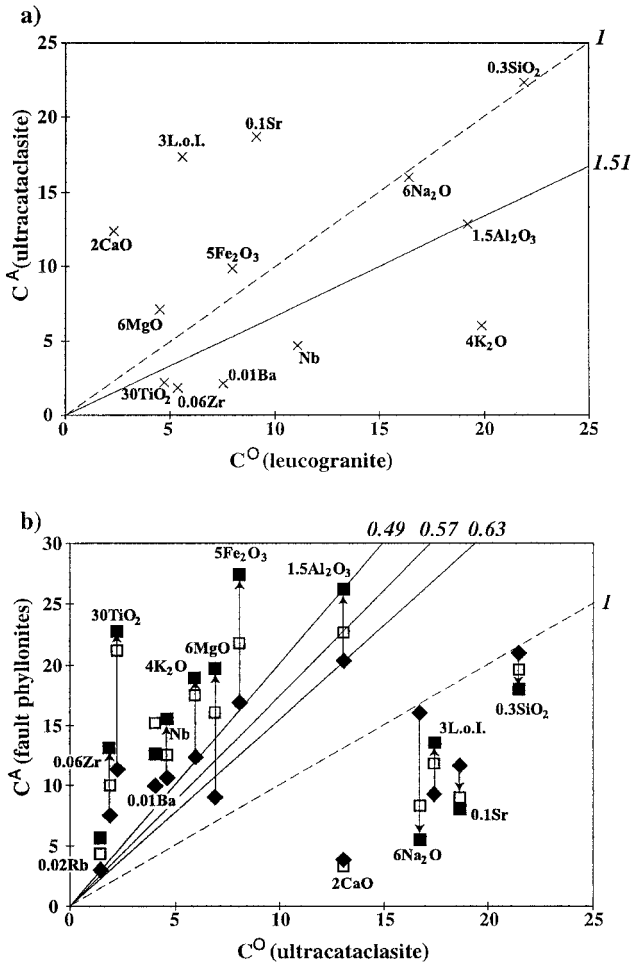


Fig. 3. Grant plots for the major element oxide and trace element data, showing relative element concentrations in the least altered and fault-rock samples. (a) Leucogranite (series D average) alteration to Vallon Fault zone cemented ultracataclasite (average of samples B1 and B2), and (b) cemented ultracataclasite alteration to phyllonites. Key: filled diamonds = phyllonite sample B5 with least well-developed cleavage (oriented 35° to the fault zone contacts); open squares = average of phyllonite samples B4 and B6 with 'moderate cleavage' (oriented 25° to the fault zone contacts); filled squares = phyllonite sample B3 with the best developed cleavage (oriented 10° to the fault zone contacts).

### 4.1. Isocon diagrams

Altered fault-rock compositions are compared to least altered equivalent compositions in order to understand the geochemical trends during the evolution of the different fault-rock types, considering possible volume changes during the reactions (Gresens, 1967). This work is based on the adaptation of the Gresens (1967) method by Grant (1986). Fig. 3 shows the concentration of major element oxides (weight percents) and trace elements (p.p.m.) in the deformed fault zone samples plotted against those of the protoliths. From these diagrams, a knowledge of the gains and losses of different elements during the evolution from protolith to fault rock may be obtained if the change in volume is known. However, volume factors are rarely known from external constraints, and in upper crustal fault zones where a significant proportion of the deformation was accommodated by cataclasis, volume changes (usually reduction) can be high (e.g. Goddard and Evans, 1995). Instead, a volume factor may be estimated from the behaviour of 'known' (or assumed) immobile elements. In Fig. 3, lines of no gains or losses (isocons) are drawn assuming aluminium immobility as is commonly the case in granitic deformation zones (e.g. Marquer, 1989) although in cataclastic fault zones this is not always the case (e.g. Goddard and Evans, 1995). For ultracataclasite formation (Fig. 3a) this assumption is probably reasonable, bearing in mind $TiO_2$ (often immobile) changes concentration in proportion with $Al_2O_3$—a volume factor of 1.51 was estimated in this case. For phyllonite formation (Fig. 3b), this assumption is more approximate (yet invoking $TiO_2$ immobility would imply unfeasibly high volume losses)—volume factors decreasing from 0.63 to 0.49 with increasing deformation were estimated.

Using these estimated volume factors, mass gains and losses may be calculated for the different fault zone alteration processes. These have been done quantitatively by Wibberley (1995); a qualitative summary is presented here. From Fig. 3(a), the alteration of least altered equivalent to cemented ultracataclasite was accompanied by:

1. a 51% gain in volume;
2. relatively large gains in Si, Na, Fe, Ca, Mg and L.O.I.;
3. relatively large loss of K.

From Fig. 3(b), the progressive alteration of ultracataclasite to well developed phyllonite was accompanied by:

1. a progressive volume loss to 49% of the original volume;
2. progressive gains of Fe and K, and some gain of Mg;
3. progressive losses of Si and Na;
4. loss in L.O.I., which becomes progressively less with increasing deformation.

Clearly, these alteration processes are very different. Common gains in Fe and Mg can be related to the growth of chlorite and iron oxide. However, the difference in volume change, and in the behaviours of Si, Na, and K, require further investigation. In the light of the microstructural observations suggesting that muscovite growth at the expense of orthoclase and albite feldspars was the most important geochemical process affecting these samples, an analysis of Na and K compositions is undertaken by comparing actual

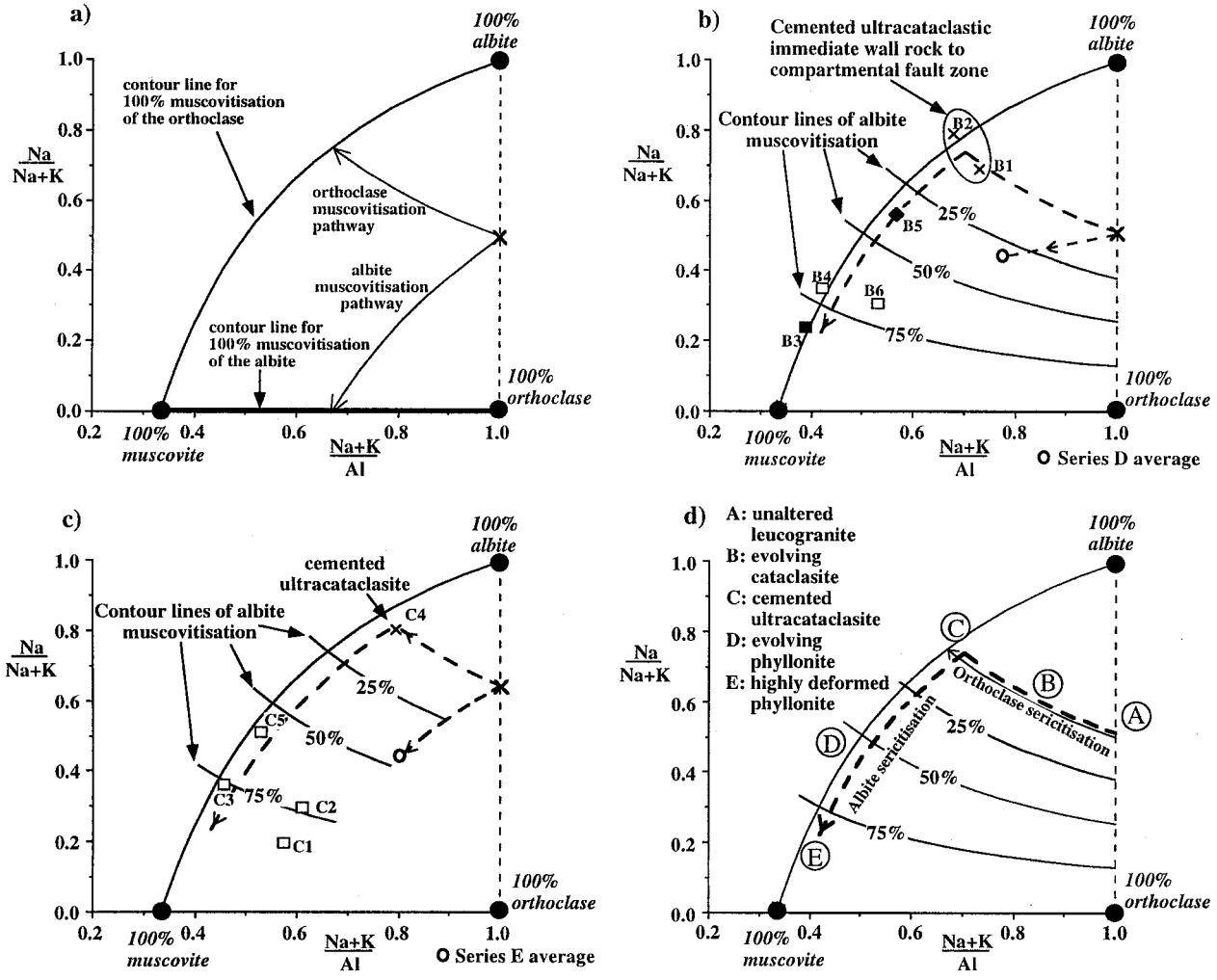


Fig. 4. Summary Na/(Na + K) vs (Na + K)/Al plots of fault-rock compositions (from Wibberley, 1995). (a) Modelled curves for muscovitisation of orthoclase or albite, using an initial composition of 50% orthoclase, 50% albite, 0% muscovite as an example. (b) Data from Vallon Fault zone samples (Series B), with least altered equivalents also shown (Series D). Key to fault-rock types as in Fig. 3. (c) Data from Ser Barbier thrust zone samples (Series C), with least altered equivalents (Series E). (d) Summary fault-rock geochemical evolution diagram.

changes with theoretical ones for the muscovitisation reactions [Eqs. (1) and (2)].

### 4.2. Na/(Na + K) vs (Na + K)/Al diagrams

The theoretical changes in composition occurring during muscovitisation of an orthoclase–albite system have been modelled on a plot of Na/(Na + K) vs (Na + K)/Al (Wibberley, 1995; Wibberley and McCaig, in review). The theoretical whole rock composition pathways for muscovitisation of the orthoclase component and of the albite component are illustrated in Fig. 4(a), using a 50% orthoclase, 50% albite starting composition as an example. Fig. 4(a) shows essentially that muscovitisation of the orthoclase component should move the composition up and to the left, whilst muscovitisation of the albite component should move the composition down and to the left. This technique assumes aluminium immobility and that no significant albitisation of the orthoclase has occurred (Wibberley and McCaig, in review). This modelling is then applied to composition data on the samples from the Vallon Fault [series B (see Fig. 1c)] in Fig. 4(b) and on the samples from the Ser Barbier Thrust [series C (see Fig. 1c)] in Fig. 4(c). Fig. 4(b) and (c) show similar trends in the data on composition of the different fault-rock types:

1. Cemented ultracataclasite samples have high Na/(Na + K) values;
2. Phyllonites have both lower Na/(Na + K) values and lower (Na + K)/Al values, progressing from the cemented ultracataclasite composition towards the 100% muscovite composition with increasing deformation;
3. A certain amount of albite sericitisation of the wall rocks occurred, meaning that the 'least altered

equivalent' samples do not reflect true protolith compositions.

The data on this Na/(Na + K) vs (Na + K)/Al plot are interpreted in the light of the findings in the microtextural section that the phyllonite forms by breakdown of ultracataclasite. Fig. 4(d) shows a two-stage alteration process:

(a) Orthoclase muscovitisation occurs first, during the formation of the cemented ultracataclasites;
(b) Progressive albite muscovitisation occurs later, during the evolution of the phyllonites.

This is consistent with the fault-rock petrographic data.

## 5. Discussion

These interpretations suggest that both the deformation leading to the production of cemented ultracataclasite, and the deformation during phyllonite formation, were accompanied by feldspar muscovitisation. However, from the petrographical and chemical data and these interpretations, two important differences exist in the generation of these two fault-rock types:

1. The feldspar being consumed was orthoclase during cemented ultracataclasite formation but albite during phyllonite formation.
2. Volume increase and Si gain accompanied cemented ultracataclasite formation whereas volume decrease and Si loss accompanied phyllonite formation.

The first difference may be explained by a change in fluid chemistry in relation to the stability fields of orthoclase, albite and muscovite, or alternatively, a change in temperature moving the stability fields with respect to a fixed fluid composition (as discussed by Wintsch, 1975a; Wintsch et al., 1995). The second difference probably relates to the behaviour of silica at each step in the geochemical and microstructural evolution. A reasonable proposition is that silica released by orthoclase muscovitisation during ultracataclasite formation migrated locally and reprecipitated in voids created as cataclastic fragments translated, rotated, and continued to fracture. Quartz precipitation in voids which developed during cataclastic breakdown of quartzo-feldspathic material is a commonly invoked cementation mechanism (e.g. Knipe, 1992; Lloyd and Knipe, 1992). This contrasts with the formation of the phyllonite, where silica released by muscovitisation was not precipitated locally but presumably remained dissolved in the fluid and was transported along the fault during fluid flow. A key difference is therefore the fate of the silica released by the muscovitisation reactions.

The findings on ultracataclasite formation illustrate how deformation mechanisms and geochemical processes are both important in governing continued fault-rock rheology and permeability. Whilst cataclastic fragmentation increased permeability, the grain-scale dilatency encouraged quartz precipitation (also discussed by Cox and Etheridge, 1989); whilst orthoclase muscovitisation released silica, silica precipitated in these dilatant sites would have increased the fault-rock strength by cement hardening, and reduced permeability (also shown by Géraud et al., 1995). In this example, the most important mechanisms are the muscovitisation reaction providing the *source* of the cement, the fragmentation providing the *pathway* for silica migration, and the grain-scale dilatancy associated with cataclastic deformation which provided the *sink* for the cement.

Further deformation, possibly initiating in regions where quartz cementation was least affected, resulted in phyllonite formation. This probably firstly occurred by fracture breakdown of the cemented cataclasite and granular sliding which increased permeability again. Then, as fluid infiltration encouraged further muscovitisation, weakening occurred with ductile deformation mechanisms operating on the newly formed aligned muscovite. In this case the silica released by the muscovitisation was mobile. Clearly the silica solubility of the fluid had increased, caused possibly by increases in pressure and temperature (Walther and Orville, 1983) or because local fluid pressures in the ultracataclasite were lower due to more dilatant site generation (Yardley and Bottrell, 1992). The reactivities of the phases undergoing alteration will depend upon their stability in $(a_{Na^+}/a_{H^+})$ vs $(a_{K^+}/a_{H^+})$ activity space at a given temperature and pressure, internal strain, fluid composition and availability (permeability dependent), and the amount of grain-size reduction (e.g. Kamineni et al., 1993; Wigum, 1995). Hence the ultimate control driving these processes is the relationship between permeability and reactivity of the evolving fault rocks with respect to the fault zone fluid. Deformation mechanism paths used to describe evolving fault rocks have illustrated the dependence of deformation mechanism history (and consequent fault zone rheology) on pressure, temperature, strain, strain rate and their change through time (Knipe, 1989, 1990). This 'Pteėt' path concept is appropriate when considering the fault rocks discussed here, with the addition that permeability has also been considered influential.

Cement hardening is one suggested way that geochemical reactions may result in an increase in the strength of a deforming material. Until now such a process has not been described in association with the breakdown of feldspars to muscovite. Yet in the case

of Alpine fault rocks from the Pelvoux Massif, cement hardening of ultracataclasite has occurred, despite geochemical evidence that feldspar-to-muscovite alteration has taken place. Silica loss and lack of cementation in the phyllonite domains suggest that silica migration out of these domains allowed them to deform more easily, resulting in overall reaction softening as has been documented from other basement fault zones (Evans, 1990; Mitra, 1992; Wibberley, 1995; Wintsch et al., 1995; Imber et al., 1997).

## 6. Conclusions

Microstructural work from granitic basement fault zones in the external western Alps shows that cemented ultracataclasites and phyllonites rich in aligned fine-grained muscovite are present. The ultracataclasites pre-date the phyllonites in the microstructural evolution of the fault zones. Petrographic and geochemical analyses of the different fault rocks suggest that formation of the cemented ultracataclasites was accompanied by volume gain, orthoclase muscovitisation and quartz precipitation, whereas formation of the phyllonite from the earlier ultracataclasite was associated with volume loss, albite muscovitisation and silica removal. These muscovitisation reactions are generally documented as reaction-softening processes. In this example however, during cataclasis, silica released in orthoclase muscovitisation precipitated locally as quartz to cement-harden the ultracataclasite. Both the deformation mechanisms associated with cataclasis, and the reactions themselves, are important in this process. Zones which continued to deform also underwent albite muscovitisation (progressively consuming albite with increasing deformation) and continued to evolve into phyllonite with reaction-softening probably the dominant strength-controlling mechanism. Hence both hardening and softening may result from feldspar to muscovite alteration in granitic fault zones, probably depending on the behaviour of silica released in the reactions. This work suggests that the effect of feldspar muscovitisation on fault rheology is more complicated than often assumed, and points to an understanding of the interplay between permeability, silica mobility and deformation mechanisms as a crucial goal for further research.

## Acknowledgements

The work was carried out whilst the author was in receipt of a NERC postgraduate studentship at Leeds University. Feedback from Rob Knipe who helped especially with TEM work, and from Andy McCaig, Rob Butler and other staff at Leeds is acknowledged. I am also grateful to Andy Grey for the XRF analyses. Thorough reviewing by Laurel Goodwin and Jim Evans greatly improved the text.

## References

Barféty, J.-C., Montjuvent, G., Pécher, A., Carme, F., 1988. Carte géologique de la France à 1/50 000. Feuille La Mure. BRGM, Orléans.

Bell, I.A., Wilson, C.J.L., 1981. Deformation of biotite and muscovite: TEM microstructure and deformation model. Tectonophysics 78, 201–228.

Brodie, K.H., Rutter, E.H., 1985. On the relationship between deformation and metamorphism with special reference to the behaviour of basic rocks. In: Thompson, A.B., Rubie, B.C. (Eds.), Advances in Physical Geochemistry, vol. 4. Springer-Verlag, Berlin, pp. 138–179.

Cox, S.F., Etheridge, M.A., 1989. Coupled grain-scale dilatancy and mass transfer during deformation at high fluid pressures: examples from Mount Lyell, Tasmania. Journal of Structural Geology 11, 147–162.

Evans, J.P., 1990. Textures, deformation mechanisms, and the role of fluids in the cataclastic deformation of granitic rocks. In: Knipe, R.J., Rutter, E.H. (Eds.), Deformation Mechanisms, Rheology and Tectonics. Geological Society Special Publication 54, pp. 29–39.

Evans, J.P., Chester, F.M., 1995. Fluid–rock interaction and weakening of faults of the San Andreas system: inferences from San Gabriel fault-rock geochemistry and microstructures. Journal of Geophysical Research 100, 13007–13020.

Frey, M., Hunzeker, J.C., Frank, W., Bocquet, J., Dal Piaz, G.V., Jäger, E., Niggli, E., 1974. Alpine metamorphism of the Alps. Schweizerische Mineralogische und Petrographische Mitteilungen 51, 247–289.

Géraud, Y., Caron, J.-M., Faure, P., 1995. Porosity network of a ductile shear zone. Journal of Structural Geology 17, 1757–1769.

Goddard, J.V., Evans, J.P., 1995. Chemical changes and fluid–rock interaction in faults of crystalline thrust sheets, northwestern Wyoming, U.S.A. Journal of Structural Geology 17, 533–547.

Grant, J.A., 1986. The isocon diagram—a simple solution to Gresens' equation for metasomatic alteration. Economic Geology 81, 1976–1982.

Gresens, R.L., 1967. Composition–volume relations of metasomatism. Chemical Geology 2, 47–65.

Hemley, J.J., Jones, W.R., 1964. Chemical aspects of hydrothermal alteration with emphasis on hydrogen metasomatism. Economic Geology 59, 538–569.

Imber, J., Holdsworth, R.E., Butler, C.A., Lloyd, G.E., 1997. Fault zone weakening processes along the reactivated Outer Hebrides Fault Zone, Scotland. Journal of the Geological Society 154, 105–109.

Janecke, S.U., Evans, J.P., 1988. Feldspar-influenced rock rheologies. Geology 16, 1064–1067.

Jullien, M., Goffé, B., 1993. Cookeite and pyrophyllite in the Dauphinois black shales (Isère, France): implications for the conditions of metamorphism in the Alpine external zones. Schweizerische Mineralogische und Petrographische Mitteilungen 73, 357–363.

Kamineni, D.C., Kerrich, R., Brown, A., 1993. Effects of differential reactivity of minerals on the development to brittle to semi-brittle structures in granitic rocks: Textural and oxygen isotope evidence. Chemical Geology 105, 215–232.

Knipe, R.J., 1989. Deformation mechanisms—recognition from natural tectonites. Journal of Structural Geology 11, 127–146.

Knipe, R.J., 1990. Microstructural analysis and tectonic evolution in thrust systems: examples from the Assynt region of the Moine Thrust Zone, Scotland. In: Barber, D.J., Meredith, P.G. (Eds.), Deformation Mechanisms in Ceramics, Minerals and Rocks. Unwin Hyman, London, pp. 228–261.

Knipe, R.J., 1992. Faulting processes and fault seal. In: Larsen, R.M., Brekke, H., Larsen, B.T., Talleraas, E. (Eds.), Structural and Tectonic Modelling and its Application to Petroleum Geology. NPF Special Publication 1, Stavanger, pp. 325–342.

Knipe, R.J., Wintsch, R.P., 1985. Heterogeneous, deformation, foliation development, and metamorphic processes in a polyphase mylonite. In: Thompson, A.B., Rubie, D.C. (Eds.), Advances in Physical Chemistry, vol. 4. Springer-Verlag, New York, pp. 180–210.

Lloyd, G.E., Knipe, R.J., 1992. Deformation mechanisms accommodating faulting of quartzite under upper crustal conditions. Journal of Structural Geology 14, 127–143.

Marquer, D., 1989. Transfert de matière et déformation des granitoïdes. Aspects méthodologiques. Schweizerische Mineralogische und Petrographische Mitteilungen 69, 15–35.

Mitra, G., 1992. Deformation of granitic basement rocks along fault zones at shallow to intermediate crustal levels. In: Mitra, S., Fisher, G.W. (Eds.), Structural Geology of Fold and Thrust Belts. The John Hopkins University Press, Baltimore, pp. 123–144.

O'Hara, K., 1988. Fluid flow and volume loss during mylonitisation: an origin for phyllonite in an overthrust setting, North Carolina, U.S.A. Tectonophysics 156, 21–36.

Rubie, D.C., 1990. Mechanisms of reaction-enhanced deformability in minerals and rocks. In: Barber, R.J., Meredith, P.G. (Eds.), Deformation Mechanisms of Ceramics, Minerals and Rocks. Unwin Hyman, London, pp. 262–295.

Shea, W.T.J., Kronenberg, A.K., 1993. Strength and anisotropy of foliated rocks with varied mica contents. Journal of Structural Geology 15, 1097–1121.

Tullis, J., 1983. Deformation of feldspars. In: Ribbe, T.H. (Ed.), Feldspar Mineralogy. Reviews in Mineralogy, vol. 2, pp. 297–322.

Voll, G., 1976. Recrystallization of quartz, biotite and feldspars from Erstfeld to the Leventina Nappe, Swiss Alps, and its geological significance. Schweizerische Mineralogische und Petrographische Mitteilungen 56, 641–647.

Walther, J.V., Orville, P.M., 1983. The extraction–quench technique for determination of the thermodynamic properties of solute complexes: application to quartz solubility in fluid mixtures. American Mineralogist 68, 731–741.

White, S.H., Knipe, R.J., 1978. Transformation and reaction enhanced ductility in rocks. Journal of the Geological Society of London 135, 513–516.

Wibberley, C.A.J., 1995. Basement involvement and deformation in Foreland Thrust Belts. Unpublished PhD thesis, Leeds, UK.

Wibberley, C.A.J., 1997. A mechanical model for the reactivation of compartmental faults in basement thrust sheets, Muzelle region, Western Alps. Journal of the Geological Society of London 154, 123–128.

Wigum, B.J., 1995. Examination of microstructural features of Norwegian cataclastic rocks and their use for predicting alkali-reactivity in concrete. Engineering Geology 40, 195–214.

Wintsch, R.P., 1975a. Solid–fluid equilibria in the system $KAlSi_3O_8$–$NaAlSi_3O_8$–$Al_2SiO_5$–$SiO_2$–$H_2O$–HCl. Journal of Petrology 16, 57–79.

Wintsch, R.P., 1975b. Feldspathisation as a result of deformation. Bulletin of the Geological Society of America 85, 35–38.

Wintsch, R.P., 1978. A chemical approach to the preferred orientation of mica. Bulletin of the Geological Society of America 89, 1715–1718.

Wintsch, R.P., Christoffersen, R., Kronenberg, A.K., 1995. Fluid–rock reaction weakening of fault zones. Journal of Geophysical Research 100, 13021–13032.

Yardley, B.W.D., Bottrell, S.H., 1992. Silica mobility and fluid movement in metamorphism of the Connemara schists, Ireland. Journal of Metamorphic Geology 10, 453–464.